(CIJST) 3007-3847 (Online) Vol. 1(2)

CAVENDISH INTERNATIONAL JOURNAL OF SCIENCE AND TECHNOLOGY

RESEARCH ARTICLE

MODELING THE TRANSMISSION DYNAMICS OF ANTHRAX DISEASE USING FRACTIONAL ORDER COMPARTMENTAL MODEL AND PHYSICS-INFORMED NEURAL NETWORKS

Open Access

Vol. 1(2):

https://journals.cavendish.ac.ug/index.php/cjst/article/view/53/32

December, 2024

Samuel Shikaa, Richard Taparki, Nicholas Ejobu*
Department of Mathematics/Statistics, Taraba State University, Jalingo, Nigeria

Abstract

Background: This research investigates the transmission dynamics of Anthrax, a zoonotic infectious disease caused by *Bacillus anthracis* bacteria, with implications for both human and livestock populations.
Methods: It employs a novel integration of mathematical modeling and physics-informed neural networks; the study provides a comprehensive analysis of Anthrax spread dynamics. Fractional differential equations are formulated within the model to capture the intricate interactions governing disease transmission, considering both quantitative and qualitative aspects. Special attention is given to the examination of steady-state solutions, particularly the local asymptotic stability of the disease-free equilibrium and its associated epidemic basic reproduction number.
Results: The analysis suggests that the model performs well in predicting variables H3 (Recovered humans), V1 (Susceptible livestock), V3 (Vaccinated livestock), and V4 (Recovered livestock), while variables H2 (Infected humans) and V2 (Infected livestock) may require further investigation or model improvement to enhance predictive performance.
Conclusion: This study contributes to advancing our understanding of Anthrax transmission dynamics and underscores the importance of interdisciplinary approaches in addressing infectious disease spread. The insights gained have significant implications for public health strategies aimed at Anthrax prevention and control.

Keywords: *Anthrax; Physics-informed Neural Networks(PINNs); Fractional Order Models; Epidemic Diseases*

INTRODUCTION

Anthrax is an acute zoonotic disease caused by a bacterium called Bacillus anthracis (Dassanayake, Khoo, & An 2021). The disease is commonly known to affect the animal population both wild and domestic (Ruiz-Fons, Segalés, & Gortázar 2008). Particularly, the herbivorous set of animals the likes of sheep, goats, cattle, and horses tend to be more exposed with a very low resistance to the disease while animals like cats, dogs and birds have considerable resistance to the disease (Van Soest, 2018). Humans are also susceptible to anthrax disease; hence, if they are exposed, they can be infected by coming in contact with animals that are infected or the products of animals that are infected (Misgie, Atnaf & Surafel, 2015).

Fractional calculus is the field of mathematical analysis that deals with investigating and applying integrals and derivatives of arbitrary order. The term fractional is a misnomer but is retained following the prevailing use. Fractional calculus may be considered an old and yet novel topic. It is an old topic since, starting from some speculations of G.W. Leibniz (1695, 1697) and L. Euler (1730), it has been developed up to nowadays. The idea of generalizing the notion of derivative to non-integer order, in particular to the order $\frac{1}{2}$, is contained in the correspondence of Leibniz with Bernoulli, L'Hospital and Wallis. Euler took the first step by observing that the result of the evaluation of the derivative of the power function has a meaning for non-integer order, thanks to his Gamma function. In recent years, fractional-order differential equations have become an important tool in mathematical modelling. Although there are many possible generalizations, $\frac{d^n}{dt^n} f\,(t)$, the most commonly used definitions are Riemann–Louville and Caputo fractional derivatives. The former concept is historically the first, and the theory about this concept has been established very well by now, but there are some

difficulties with applying it to real-life problems. In order to overcome these difficulties, the latter concept, Caputo type derivative, is defined. This new concept is closely related to the Riemann–Louville derivative (Mainardi & Gorenflo, 2013). Demirci and Ozalp, (2012) considered the nonlinear Caputo-type fractional differential equations of order $0 < \alpha < 1$, which are used in modeling physical and biological facts. In most of these techniques, either the solutions of integer order differential equation versions of the given fractional differential equations or the series expansions in the neighbourhood of the initial conditions are used. Although the human contribution to the transmission of anthrax disease between animals is negligible, it becomes a very important subject to discuss the transmission of this disease in the animal population only. The fractional-order system (FDE) is related to systems with memory, history, or nonlocal effects, which exist in many biological systems that show the realistic biphasic decline behaviour of infection or diseases but at a slower rate (Rezapour, Etemad & Mohammadi, 2020).

The aim of this paper is to model the transmission dynamics of anthrax disease using a fractional compartmental model and physics-informed neural networks. This approach leverages the memory and nonlocal effects inherent in fractional calculus to provide a more accurate and realistic representation of the disease's progression within animal and human populations.

2. Background

In this section, we introduce Anthrax compartmental models both integer and fractional order.

2.1 Anthrax Model

The compartmental model adopted in this paper was inspired by Osman et al, 2018.

The model divides human and animal populations at the time (t) into seven (7) compartments with respect to their disease status in the system. In humans, there are three compartments; susceptible, infected and recovered humans while in animals there are 4 compartments; susceptible, infected, recovered and vaccinated animals. The integer order of this compartmental model of anthrax lacks the precision to capture the intricate and nuanced characteristics of anthrax disease transmission. Hence, in this study, the model is modified and expressed in fractional order.

2.1.1 Schematic Diagram

The total livestock population, $V_N(t)$, is subdivided into Susceptible livestock, $V_1(t)$, Infected livestock, $V_2(t)$, Vaccinated livestock, $V_3(t)$ and Recovered livestock, $V_4(t)$. Hence, the total livestock population is as follows.

$$V_N(t) = V_1(t) + V_2(t) + V_3(t) + V_4(t) \quad (1)$$

Similarly, the total human population, $H_N(t)$, is subdivided into Susceptible humans, $H_1(t)$, Infected humans, $H_2(t)$ and Recovered humans, $H_3(t)$. Hence, the total human population is as follows.

$$H_N(t) = H_1(t) + H_2(t) + H_3(t) \quad (2)$$

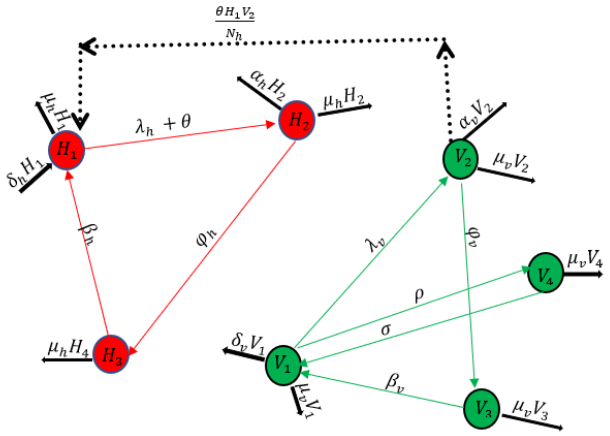

Figure 1: Schematic diagram of anthrax transmission between humans and livestock

2.1.2 Integer order of the model

From Figure 1, a system of integer-order ordinary differential equations is presented as follows.

$$\left.\begin{aligned}
\frac{dH_1}{dt} &= \delta_h N_h - \left(\frac{\lambda_h H_2 + \theta V_2}{N_h} + \mu_h\right) H_1 + \beta_h H_3 \\
\frac{dH_2}{dt} &= \left(\frac{\lambda_h H_2 + \theta V_2}{N_h}\right) H_1 - (\mu_h + \alpha_h + \varphi_h) H_2 \\
\frac{dH_3}{dt} &= \varphi_h H_2 - (\mu_h + \beta_h) H_3 \\
\frac{dV_1}{dt} &= \delta_v N_v - \frac{\lambda_v V_1 V_2}{N_v} - \mu_v V_1 + \beta_v V_3 - \rho V_1 + \sigma V_4 \\
\frac{dV_2}{dt} &= \frac{\lambda_v V_1 V_2}{N_v} - (\mu_v + \varphi_v + \alpha_v) V_2 \\
\frac{dV_3}{dt} &= \varphi_v V_2 - (\mu_v + \beta_v) V_3 \\
\frac{dV_4}{dt} &= \rho V_1 - \sigma V_4
\end{aligned}\right\} \quad (3)$$

subject to the initial conditions.

$$V_1(0) \geq 0,\ V_2(0) \geq 0,\ V_3(0) \geq 0,\ V_4(0) \geq 0;$$

$$H_1(0) \geq 0, H_2(0) \geq 0, H_3(0) \geq 0, H_5(0) \geq 0$$

2.1.3 Fractional order of the model

From system (3), the corresponding fractional order system of the Caputo type derivative is as follows.

$$
\begin{aligned}
{}_0^C D_t^{\alpha_1} H_1(t) &= \delta_h N_h - \left(\frac{\lambda_h H_2 + \theta V_2}{N_h} + \mu_h\right) H_1 + \beta_h H_3 \\
{}_0^C D_t^{\alpha_2} H_2(t) &= \left(\frac{\lambda_h H_2 + \theta V_2}{N_h}\right) H_1 - (\mu_h + \alpha_h + \varphi_h) H_2 \\
{}_0^C D_t^{\alpha_3} H_3(t) &= \varphi_h H_2 - (\mu_h + \beta_h) H_3 \\
{}_0^C D_t^{\alpha_4} V_1(t) &= \delta_v N_v - \frac{\lambda_v V_1 V_2}{N_v} - \mu_v V_1 + \beta_v V_3 - \rho V_1 + \sigma V_4 \\
{}_0^C D_t^{\alpha_5} V_2(t) &= \frac{\lambda_v V_1 V_2}{N_v} - (\mu_v + \varphi_v + \alpha_v) V_2 \\
{}_0^C D_t^{\alpha_6} V_3(t) &= \varphi_v V_2 - (\mu_v + \beta_v) V_3 \\
{}_0^C D_t^{\alpha_7} V_4(t) &= \rho V_1 - \sigma V_4
\end{aligned}
\tag{4}
$$

with initial conditions.

$$V_1(0) \geq 0,\ V_2(0) \geq 0,\ V_3(0) \geq 0,\ V_4(0) \geq 0;$$

$$H_1(0) \geq 0, H_2(0) \geq 0, H_3(0) \geq 0$$

where ${}_0^C D_t^{\alpha_i}$ symbolizes the Caputo type fractional derivative of order $\alpha,\ 0 < \alpha \leq 1$ with respect to t;

$${}_a^C D_t^{\alpha} \mathrm{f(t)} = \frac{1}{\Gamma(n-\alpha)} \int_a^t (t-\tau)^{n-\alpha-1} f^{(n)}(\tau) d\tau$$

$n - 1 < \alpha < n$

The parameters of the model are defined as follows.

δ_h = recruitment rate in the human population
δ_v = recruitment rate in the livestock population
α_h = rate at which infected humans die of Anthrax
α_v = rate at which infected livestock die of Anthrax
β_h = rate at which recovered humans lose immunity and become susceptible again
β_v = rate at which recovered livestock lose immunity and become susceptible again
λ_h = rate of infection from human-to-human population
θ = rate of infection from animal to human population
λ_v = rate of infection in livestock population
μ_h = rate at which natural death occurs in the human population
μ_v = rate at which natural death occurs in the livestock population
φ_h = rate at which infected humans recover from the disease
φ_v = rate at which infected livestock recover from anthrax disease
σ = rate at which vaccinated livestock become susceptible due to loss of immunity
ρ = proportion of livestock vaccinated

2.2 Analysis of the Model

The analysis of system (4) will be carried out. First, the steady states of the system are determined, the disease-free and endemic equilibrium points in other words. Hence, the analysis of the equilibrium points is carried out to determine the stability of the fractional order model.

2.2.1 Equilibrium points of the fractional order model

There are two equilibrium points: the Disease-Free Equilibrium (DFE) and the Endemic Equilibrium (EE) point. To obtain these, system (4) is equated to zero and solved homogeneously as follows.

$${}_0^C D_t^{\alpha_1} H_1(t) = {}_0^C D_t^{\alpha_2} H_2(t) = {}_0^C D_t^{\alpha_3} H_3(t)$$

$$= {}_0^C D_t^{\alpha_4} V_1(t) = {}_0^C D_t^{\alpha_5} V_2(t) = {}_0^C D_t^{\alpha_6} V_3(t)$$

$$= {}_0^C D_t^{\alpha_7} V_4(t) = 0$$

When the disease is not present it implies there are no infections and recovery. Hence, the disease-free equilibrium can be obtained as follows.

$$\delta_h N_h - \left(\frac{\lambda_h H_2 + \theta V_2}{N_h} + \mu_h\right) H_1 + \beta_h H_3 = 0 \tag{5}$$

$$\delta_v N_v - \frac{\lambda_v V_1 V_2}{N_v} - \mu_v V_1 + \beta_v V_3 - \rho V_1 + \sigma V_4 = 0 \tag{6}$$

$$\rho V_1 - \sigma V_4 = 0 \tag{7}$$

From (5) since there is no infection, we have that;

$$\delta_h N_h - \mu_h H_1 = 0$$

$$\delta_h N_h = \mu_h H_1$$

$$\therefore H_1 = \frac{\delta_h N_h}{\mu_h} = H_1^*$$

From (6) since there is no infection, we have that;

$$\delta_v N_v - (\mu_v + \rho) V_1 + \sigma V_4 = 0 \tag{8}$$

From (7);

$$V_4 = \frac{\rho V_1}{\sigma} \tag{9}$$

Substituting (9) in (8);

$$\delta_v N_v - (\mu_v + \rho) V_1 + \sigma \left(\frac{\rho V_1}{\sigma}\right) = 0$$

$$\delta_v N_v - (\mu_v + \rho) V_1 + \rho V_1 = 0$$

$$\delta_v N_v - \mu_v V_1 - \rho V_1 + \rho V_1 = 0$$

$$\delta_v N_v - \mu_v V_1 = 0$$

Hence.

$$V_1 = \frac{\delta_v N_v}{\mu_v} = V_1^*$$

This implies that;

$$V_4 = \frac{\rho}{\sigma}\left(\frac{\delta_v N_v}{\mu_v}\right) = V_4^*$$

Hence,

$$\mathrm{DFE} = (H_1^*, H_2^*, H_3^*, V_1^*, V_2^*, V_3^*, V_4^*) = \left(\frac{\delta_h N_h}{\mu_h}, 0, 0, \frac{\delta_v N_v}{\mu_v}, 0, 0, \frac{\rho}{\sigma}\left(\frac{\delta_v N_v}{\mu_v}\right)\right)$$

Obtaining the endemic equilibrium point for system (5), the basic reproduction number (R_0) is determined using the next-generation matrix. The basic reproduction number is the threshold parameter that governs the spread of a disease. The next generation matrix is defined as; $K = FP^{-1}$ and $R_0 = \tau(FP^{-1})$ where $\tau(FP^{-1})$ denotes the spectral radius of $\tau(FP^{-1})$. The basic reproduction number R_0, is defined as the spectral radius of the next-generation matrix. The

spectral radius of a matrix A is defined as the maximum of the absolute values of the eigenvalues of the matrix.

$A: \tau(A) = sup\{|\varepsilon|\}: \varepsilon \in \tau(A)$ where $\tau(A)$ represents the set of eigen values of the matrix A.

Considering only the infective compartments of the system (5);

$$ {}_0^C D_t^{\alpha_2} H_2(t) = \left(\frac{\lambda_h H_2 + \theta V_2}{N_h}\right) H_1 - (\mu_h + \alpha_h + \varphi_h) H_2 \quad (10) $$

$$ {}_0^C D_t^{\alpha_5} V_2(t) = \frac{\lambda_v V_1 V_2}{N_v} - (\mu_v + \varphi_v + \alpha_v) V_2 \quad (11) $$

Let $F = \begin{bmatrix} \left(\frac{\lambda_h H_2 + \theta V_2}{N_h}\right) H_1 \\ \frac{\lambda_v V_1 V_2}{N_v} \end{bmatrix}$,

$$ P = \begin{bmatrix} -(\mu_h + \alpha_h + \varphi_h) H_2 \\ -(\mu_v + \varphi_v + \alpha_v) V_2 \end{bmatrix} $$

Let F and P be represented by;

$$ F = \begin{bmatrix} \frac{\partial f_1}{\partial H_2} & \frac{\partial f_1}{\partial V_2} \\ \frac{\partial f_2}{\partial H_2} & \frac{\partial f_2}{\partial V_2} \end{bmatrix} = \begin{bmatrix} \frac{\lambda_h H_1}{N_h} & \frac{\theta H_1}{N_h} \\ 0 & \frac{\lambda_v V_1}{N_v} \end{bmatrix} \quad (12) $$

$$ P = \begin{bmatrix} \frac{\partial f_1}{\partial H_2} & \frac{\partial f_1}{\partial V_2} \\ \frac{\partial f_2}{\partial H_2} & \frac{\partial f_2}{\partial V_2} \end{bmatrix} $$

$$ = \begin{bmatrix} -(\mu_h + \alpha_h + \varphi_h) & 0 \\ 0 & -(\mu_v + \varphi_v + \alpha_v) \end{bmatrix} \quad (13) $$

Substituting the DFE into equation (12)

$$ F = \begin{bmatrix} \frac{\lambda_h H_1^*}{N_h} & \frac{\theta H_1^*}{N_h} \\ 0 & \frac{\lambda_v V_1^*}{N_v} \end{bmatrix} \quad (14) $$

Taking the inverse of equation (13), it becomes.

$$ P^{-1} = \begin{bmatrix} -\frac{1}{\mu_h + \alpha_h + \varphi_h} & 0 \\ 0 & -\frac{1}{\mu_v + \varphi_v + \alpha_v} \end{bmatrix} \quad (15) $$

$$ FP^{-1} = \begin{bmatrix} -\frac{\lambda_h H_1^*}{(\mu_h + \alpha_h + \varphi_h) N_h} & -\frac{\theta H_1^*}{(\mu_v + \varphi_v + \alpha_v) N_h} \\ 0 & -\frac{\lambda_v V_1^*}{(\mu_v + \varphi_v + \alpha_v) N_v} \end{bmatrix} \quad (16) $$

The eigenvalue matrix is given as follows;

$$ \begin{bmatrix} -\frac{\lambda_h H_1^*}{(\mu_h + \alpha_h + \varphi_h) N_h} - A & -\frac{\theta H_1^*}{(\mu_v + \varphi_v + \alpha_v) N_h} \\ 0 & -\frac{\lambda_v V_1^*}{(\mu_v + \varphi_v + \alpha_v) N_v} - A \end{bmatrix} = 0 \quad (17) $$

$$ A^2 - \left\{\left(\frac{\lambda_h H_1^*}{(\mu_h + \alpha_h + \varphi_h) N_h}\right) + \left(\frac{\lambda_v V_1^*}{(\mu_v + \varphi_v + \alpha_v) N_v}\right)\right\} A = 0 \quad (18) $$

Hence,

$A = 0$ or $A = \left(\frac{\lambda_h H_1^*}{(\mu_h + \alpha_h + \varphi_h) N_h}\right) + \left(\frac{\lambda_v V_1^*}{(\mu_v + \varphi_v + \alpha_v) N_v}\right)$.

Considering the dominant eigenvalue.

$$ R_{hv} = \left(\frac{\lambda_h H_1^*}{(\mu_h + \alpha_h + \varphi_h) N_h}\right) + \left(\frac{\lambda_v V_1^*}{(\mu_v + \varphi_v + \alpha_v) N_v}\right) \quad (19) $$

Where R_h and R_v represents the reproduction numbers for human and livestock populations respectively.

Since

$$ (H_1^*, H_2^*, H_3^*, V_1^*, V_2^*, V_3^*, V_4^*) = \left(\frac{\delta_h N_h}{\mu_h}, 0, 0, \frac{\delta_v N_v}{\mu_v}, 0, 0, \frac{\rho}{\sigma}\left(\frac{\delta_v N_v}{\mu_v}\right)\right) $$

this implies that.

$$ R_h = \frac{\delta_h \lambda_h}{(\mu_h + \alpha_h + \varphi_h) \mu_h} \quad (20) $$

$$ R_v = \frac{\delta_v \lambda_v}{(\mu_v + \varphi_v + \alpha_v) \mu_v} \quad (21) $$

2.2.2 Global Stability of Disease-free and Endemic Equilibrium

The analysis of Osman et al (2018) shows that the disease-free equilibrium is globally asymptotically stable by proving that; if the disease-free equilibrium is less than one $(R_{hv} < 1)$ then it is globally asymptotically stable in the interior of $H_1, H_2, V_2 \in \Phi$. On the other hand, the endemic equilibrium only exists when $R_{hv} \leq 1$ and it is globally asymptotically stable.

3. The Algorithm

In this section, we introduce Physics-Informed Neural Networks (PINNs), a pivotal algorithm slated for utilization in simulating the dynamics of the disease. PINNs represent a sophisticated computational tool that seamlessly integrates neural networks with physical principles, thereby enabling the assimilation of domain knowledge into the learning process. By leveraging PINNs, we aim to achieve a comprehensive understanding of the underlying mechanisms governing disease transmission dynamics. This approach holds promise for enhancing predictive accuracy and capturing intricate interactions within the Anthrax transmission system, thereby bolstering the efficacy of our modelling endeavors.

3.1 Physics-Informed Neural Network

Physics-informed neural networks were first proposed by Raissi *et al* (2019). The physics-informed neural networks are neural networks that are trained to solve supervised learning tasks while respecting any given law of physics described by general nonlinear partial differential equations.

3.1.1 Formulation of Physics Informed Neural Network

Let $U(t)$ be the vector of all the compartments in the system (5), then the coupled system of differential equation governing the dynamics of that model can be written as;

$$ \Psi\, U(t) = F(U(t), \beta) \quad (22) $$

where Ψ may be integer-order or fractional-order temporal differential operator, F is a nonlinear operator and β is the set of known or unknown model parameters.

The formulation of PINNs is to construct a physics-informed deep learning algorithm to solve the forward and inverse problems involving differential equations by employing a deep neural network to approximate the unknown function. Let $NN(t, \vartheta)$ be a deep neural network having input t and parameterized by ϑ as weights and biases of the network. The solution of the differential equation is approximated by the neural network;

$$U(t) \approx NN(t, \vartheta) \quad (23)$$

The residual is defined as;

$$R_{NN}(t) = \frac{d}{dt} NN(t) - F(NN(t), \beta) \quad (24)$$

and encode this residual into the network.

3.1.2 Loss Function

Two finite sets of training points $\{t_u^i\}_{i=0}^{N_u}$ and residual points $\{t_r^i\}_{i=0}^{N_r}$ is defined. The training points are the points where data is available, and the residual points are the points where the residual $R_{NN}(t)$ is satisfied, and they are randomly selected over the entire computational domain. Hence, the loss function of PINN is given as;

$$L(\vartheta, \beta) = w_u MSE_u + w_r MSE_r \quad (25)$$

$$w_u MSE_u = w_u \frac{1}{N_u} \sum_{i=1}^{N_u} \left| NN(t_u^i) - U^D(t_u^i) \right|^2 \quad (26)$$

and

$$w_r MSE_r = w_r \frac{1}{N_u} \sum_{i=1}^{N_R} \left| \frac{d}{dt} NN(t_r^i) - F(NN(t_r^i), \beta) \right|^2 \quad (31)$$

where MSE is the mean square error. The loss function of PINN contains two terms. The MSE_u which measures the mismatch between solution $NN(t)$ and data U^D at the training points in the training set. This depends on data availability on the epidemiological classes. The other term, MSE_r penalizes the governing equation at the residual points.

3.1.3 The Schematic Diagram of Physics-Informed Neural Network

From Figure 2, layer A is the input layer with a single neuron, this layer takes in data t of the system (4) into the single neuron which will transmit to layer B. Layer B is known as the hidden layer with multiple neurons, it multiplies the data by the neurons respective weights(w), add it to the bias(b) and then activate it with an activation function (f) before transmitting the result to layer C. Layer C is also considered a hidden layer with multiple neurons, it does similar operation with layer B and what it passes to layer D (output layer with a single neuron) is the prediction of the solution of system (3.4). From here the ODEs residual is calculated and the data loss is also calculated. If epsilon (ε) is greater than the total loss then the weights are adjusted and the process is repeated otherwise the predicted solution is equivalent to the exact solution of the system.

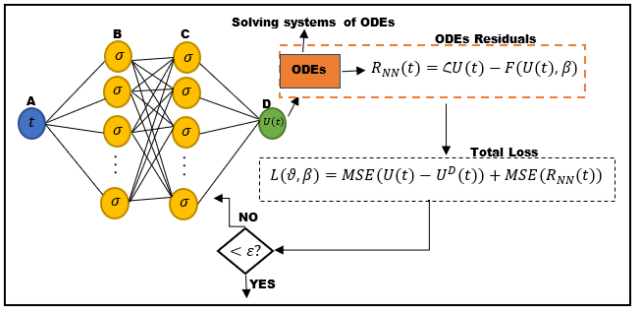

Figure 2: Schematic diagram of physics-informed neural network

4. Numerical Results and Analysis

During this research, a comprehensive dataset documenting occurrences of anthrax disease within both human and livestock populations of Nigeria was not readily available for integration into the training regimen of the Physics-informed Neural Network. In light of this scarcity, data synthesis became necessary, utilizing disease parameters sourced from pertinent literature references, as delineated in Table 1. This synthesis encompassed data pertaining to the 2024 human population of Nigeria (https://worldpopulationreview.com/countries/nigeria-population) and the livestock population (https://www.researchgate.net/figure/Nigeria-livestock-population-estimates_tbl1_3379459241/4), encompassing sheep, cattle, and goats. For the purpose of subsequent testing, fractional parameters denoted as $\alpha_1, \ldots, \alpha_7$were stipulated, as outlined in the respective table.

Table 1 Disease Parameters

Parameter	Description	Value	Reference
δ_h	recruitment rate in the human population	0.2	Osman et al, 2018
δ_v	recruitment rate in the livestock population	0.005	Osman et al, 2018
α_h	the rate at which infected humans die of Anthrax	0.2	Osman et al, 2018
α_v	the rate at which infected livestock die of Anthrax	0.45	Osman et al, 2018
β_h	rate at which recovered humans' loss immunity and become susceptible again	0.006	Osman et al, 2018
β_v	the rate at which recovered livestock loss immunity and become susceptible again	0.00005	Osman et al, 2018
λ_h	rate of infection from human-to-human population	0.00005	Assumed
θ	rate of infection from animal to human population	0.00005	Assumed
λ_v	rate of infection in the livestock population	0.00005	Osman et al, 2018
μ_h	the rate at which natural death occurs in the human population	0.0001	Osman et al, 2018
μ_v	the rate at which natural death occurs in the livestock population	0.0004	Osman et al, 2018
φ_h	the rate at which infected humans recover from the disease	0.75	Osman et al, 2018
φ_v	rate at which infected livestock recover from anthrax disease	0.0025	Osman et al, 2018
σ	rate at which vaccinated livestock become susceptible due to loss of immunity	0.002	Osman et al, 2018
ρ	the proportion of livestock vaccinated	0.0001	Osman et al, 2018

Table 2 Fractional Parameters

Parameter	Value
α_1	0.97
α_2	0.85
α_3	0.86
α_4	0.87
α_5	0.979
α_6	0.89
α_7	0.87

Upon training the model specified in equation for a total of 41,000 epochs, the ensuing results were as follows:

Figure 3: Plots of Actual and predicted values of Anthrax in the Human population compartments

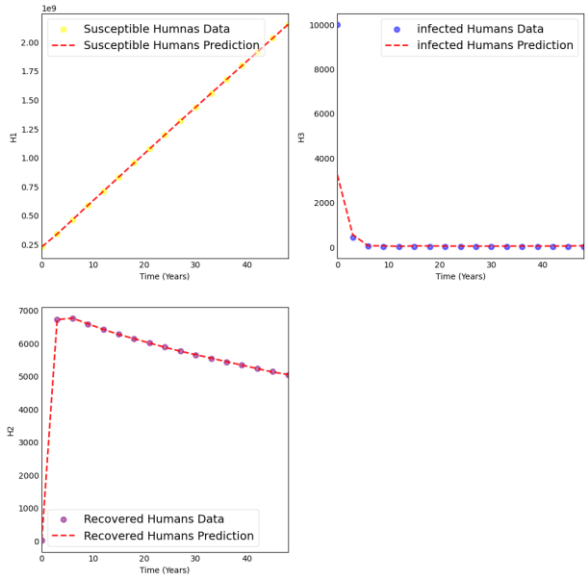

in Figure 3 the plots of Susceptible humans (H_1), Infected humans (H_2) and Recovered humans (H_3) are been presented corresponding to the predicted values.

Figure 4: Plots of Actual and predicted values of Anthrax in Livestock population compartments

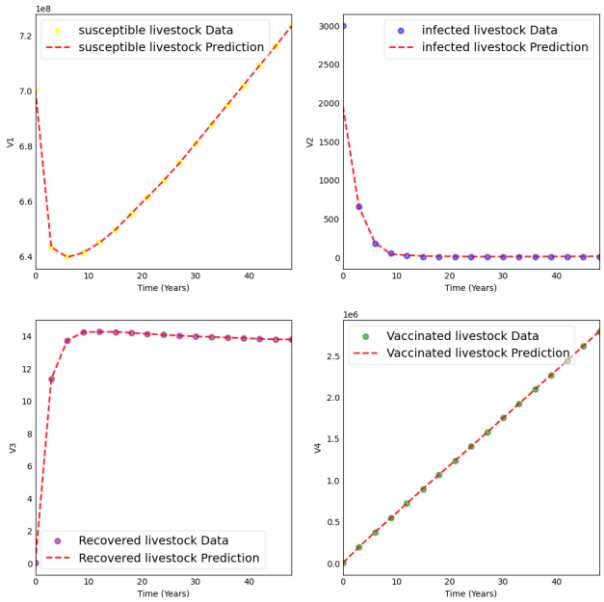

Similarly, in Figure 4, the plots of Susceptible livestock (V_1), Infected livestock (V_2), Recovered livestock (V_3) and Vaccinated livestock (V_4) are also presented. The plots correspond to the predicted values

Figure 5: Lower and Upper solution in the human population compartments

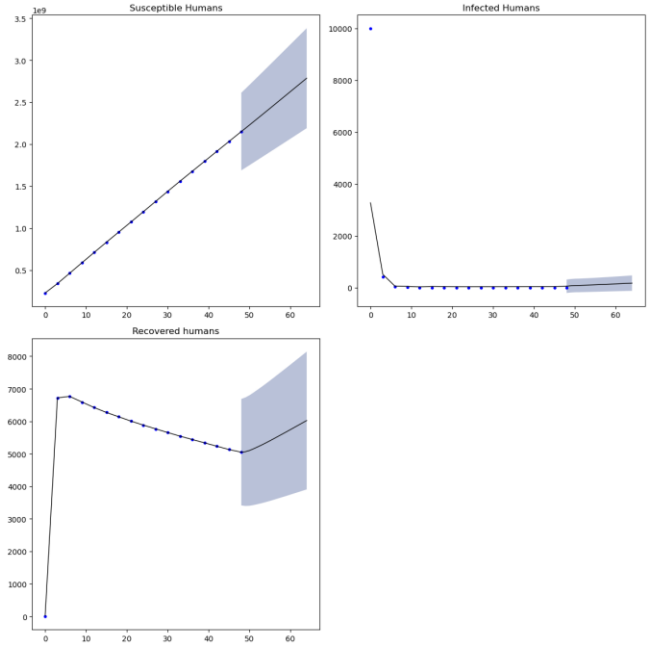

The figure illustrate the lower and upper solutions for each compartment within the human population, as referenced in Figure 5.

Figure 6: Lower and Upper solution in the livestock population compartments

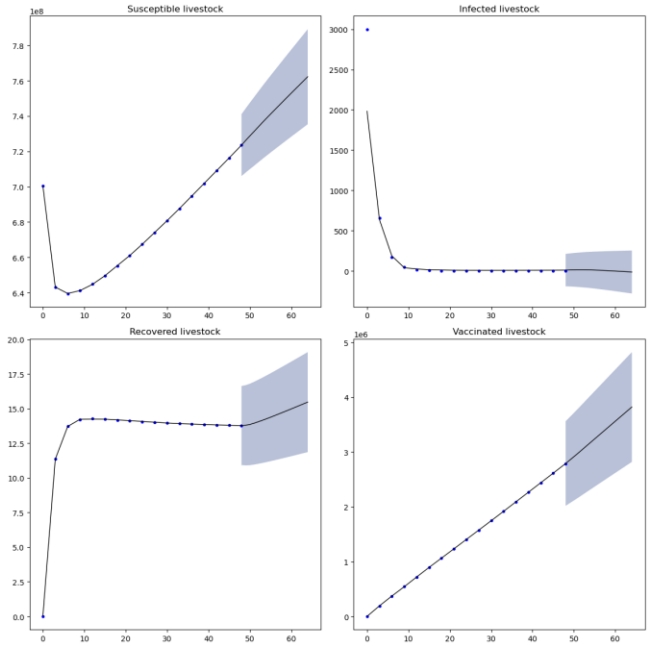

The corresponding graphical representation for the livestock population, as referenced in Figure 6, illustrates the lower and upper solutions for each compartment.

Figure 7: Future prediction of Anthrax dynamics in Human Population

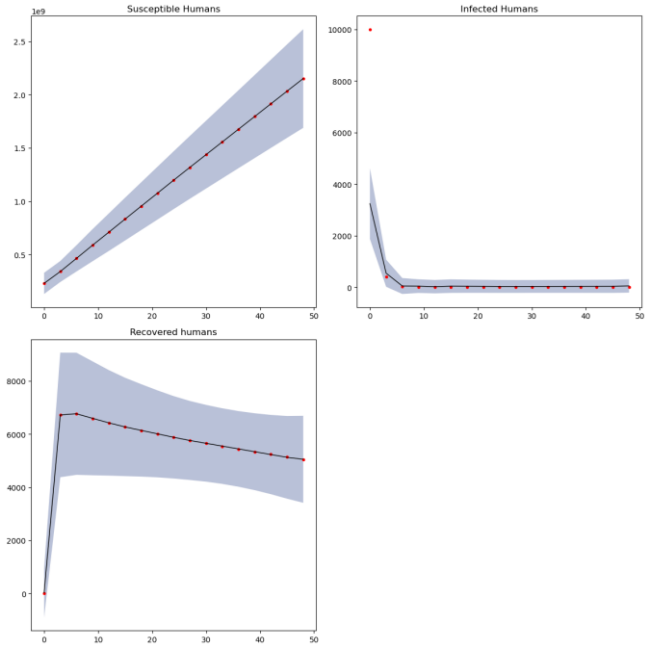

In Figure 7, a comprehensive portrayal of the anticipated future dynamics of Anthrax disease within the human population is meticulously presented, offering invaluable insights into the projected trajectory of the disease's prevalence and its potential implications.

Figure 8: Future prediction of Anthrax dynamics in Livestock Population

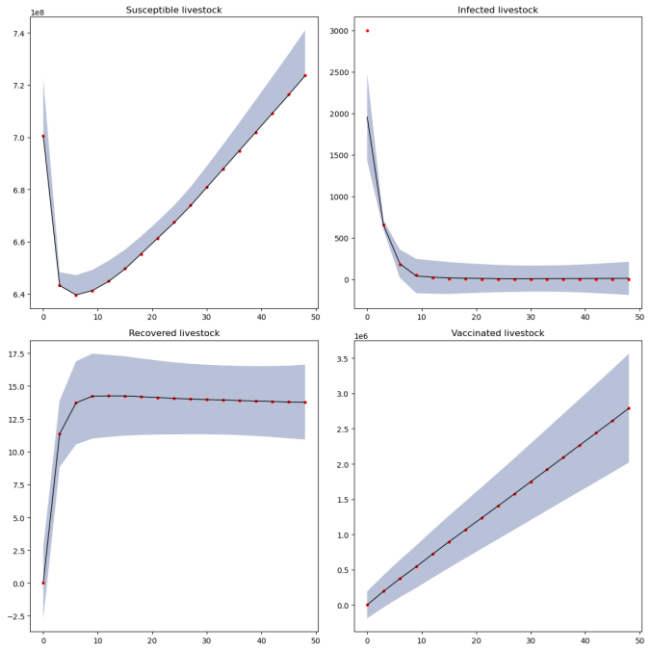

Figure 8 provides a detailed visualization of the predicted future dynamics of Anthrax disease within the livestock population. This graphical representation offers a nuanced understanding of the anticipated trends and potential implications for livestock health and management practices.

Figure 9: Estimated Fractional order Parameters

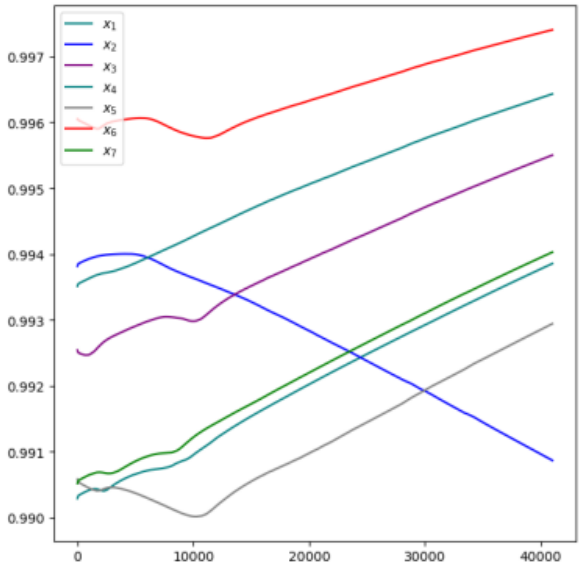

Table 4 provides evaluation metrics for different variables, including Mean Absolute Error (MAE), Root Mean Square Error (RMSE), and R-squared (R2) values.

For variable H1, the MAE and RMSE are relatively high, indicating a significant difference between predicted and actual values. However, the R2 value is close to 1, suggesting a strong correlation between predicted and actual values.

Variable H2 has lower MAE and RMSE compared to H1, indicating better model performance in terms of accuracy. However, the R2 value is relatively low, suggesting that the model explains only a moderate amount of the variance in the data.

Variable H3 has very low MAE and RMSE values, indicating excellent model accuracy. The high R2 value close to 1 suggests that the model explains almost all of the variance in the data.

Variables V1, V3, and V4 show similar patterns with very low MAE and RMSE values and high R2 values close to 1, indicating high model accuracy and good explanatory power.

Variable V2 has moderate MAE and RMSE values and a relatively lower R2 value compared to other variables, indicating moderate model accuracy and explanatory power.

Consequently, the analysis suggests that the model performs well in predicting variables H3, V1, V3, and V4, while variables H2 and V2 may require further investigation or model improvement to enhance predictive performance.

The estimations of the fractional order parameters are graphically depicted within a plot, as showcased in Figure 9, elucidating their convergence pattern across training epochs.

Figure 10: Plot of Model Loss

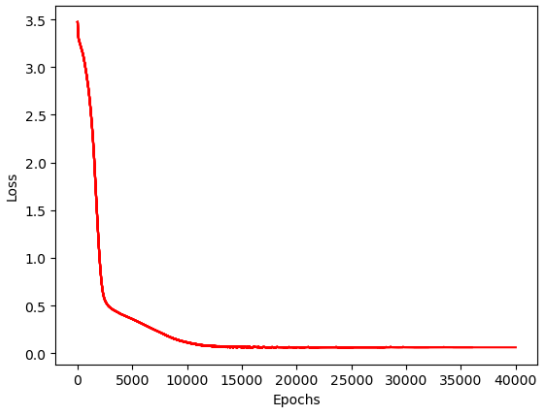

Figure 10 displays the plot of model loss, offering a visual representation of the evolution of loss values over the course of training.

Table 4: Accuracy Analysis

Variable	Mean Absolute Error	Root Mean Square Error	R-Squared (R^2)
H1	860435.198160	1.095160e+06	0.999997
H2	435.422856	1.632949e+03	0.516322
H3	3.630468	5.954185e+00	0.999984
V1	64453.642824	7.641015e+04	0.999992
V2	68.856648	2.469425e+02	0.878923
V3	0.008947	1.220064e-02	0.999986
V4	1174.344778	1.641727e+03	0.999996

5. Discussion and Conclusion

The fractional compartmental model, designed to analyze Anthrax disease transmission dynamics in both human and livestock populations, yields valuable insights into the spread of the disease. The model's results indicate notable relationships between various parameters and the transmission dynamics.

Reducing the animal recovery rate is observed to correlate with an increase in disease spread across both human and animal populations. Likewise, an increase in human recruitment rate leads to heightened disease transmission, given the absence of vaccination measures in the human population. Conversely, decreasing human and livestock recruitment rates, as well as livestock and human transmission rates, is associated with a decrease in disease transmission, slowing down its propagation.

The model's significance lies in its ability to elucidate Anthrax transmission dynamics by highlighting the collective impact of parameters across human and animal populations. The transition from the integer compartmental model proposed by Osman et al. (2018) to a fractional formulation, integrated with a physics-informed neural network, represents a notable improvement. Unlike the integer model, the fractional model delineates the specific rate of change for each compartment, providing a more detailed understanding of disease dynamics.

The convergence of fractional parameters depicted in Figure 9 indicates their predictive capacity regarding compartmental dynamics over time, achieved through training the model across multiple epochs. This convergence enhances the model's accuracy and reliability in forecasting Anthrax transmission patterns.

Anthrax is a zoonotic disease that has caused the death of many humans and livestock in the regions where it has broken out. Hence, it is essential to be aware of the outbreak of this disease, as it is still endemic in many regions. This paper illustrates how this disease interacts in both human and animal populations. The infection force originates from the livestock population and affects the human population, as anthrax disease is associated with animals, particularly herbivores like sheep, goats, and cattle. If animals are protected from this disease, the infection rate will drastically reduce, leading to the disease dying out.

References

Columba, T., & Ifedayo, A. (2023). Public Health Advisory: Anthrax outbreak in Ghana. Nigeria Centre for Disease Control and Prevention. Retrieved from https://ncdc.gov.ng/news/461/public-health-advisory%3A-anthrax-outbreak-in-ghana

Dassanayake, M. K., Khoo, T. J., & An, J. (2021). Antibiotic resistance modifying ability of phytoextracts in anthrax biological agent Bacillus anthracis and emerging superbugs: a review of synergistic mechanisms. Annals of Clinical Microbiology and Antimicrobials, 20(1), 1-36.

Demirci, E., & Ozalp, N. (2012). A method for solving differential equations of fractional order. Journal of Computational and Applied Mathematics, 236(11), 2754-2762.

Gao, K., Mei, G., Piccialli, F., Cuomo, S., Tu, J., & Huo, Z. (2020). Julia language in machine learning: Algorithms, applications, and open issues. Computer Science Review, 37, 100254.

Grant, C., Iacono, G. L., Dzingirai, V., Bett, B., Winnebah, T. R., & Atkinson, P. M. (2016). Moving interdisciplinary science forward: integrating participatory modelling with mathematical modelling of zoonotic disease in Africa. Infectious Diseases of Poverty, 5(01), 6-17.

Mainardi, F., & Gorenflo, R. (2013). Fractional calculus and special functions. Lecture Notes on Mathematical Physics, Department of Physics, University of Bologna, Italy.

Misgie, F., Atnaf, A., & Surafel, K. (2015). A review on Anthrax and its public health and economic importance. Academic Journal of Animal Diseases, 4(3), 196-204.

Osman, S., Makinde, O. D., & Theuri, D. M.

(2018). Mathematical modelling of transmission dynamics of Anthrax in human and animal population. Mathematics Theory Modelling, 8.

Raissi, M., Perdikaris, P., & Karniadakis, G. E.

(2019). Physics-informed neural networks: A deep learning framework for solving forward and inverse problems involving nonlinear partial differential equations. Journal of Computational Physics, 378, 686-707.

Rezapour, S., Etemad, S., & Mohammadi, H.

(2020). A mathematical analysis of a system of Caputo–Fabrizio fractional differential equations for the anthrax disease model in animals. Advances in Difference Equations, 2020(1), 481.

Ruiz-Fons, F., Segalés, J., & Gortázar, C. (2008).

A review of viral diseases of the European wild boar: effects of population dynamics and reservoir role. The Veterinary Journal, 176(2), 158-169.

Van Soest, P. J. (2018). Nutritional ecology of the

ruminant. Cornell University Press.